Malaysian NANO-An International Journal

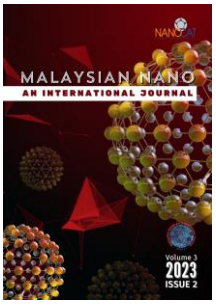

Research article

Received 21th August 2023
Revised 28th October 2023
Accepted 27th December 2023

DOI:
10.22452/mnij.vol3no2.3

Corresponding authors:
faysalkabir.dup@gmail.com
Orchid ID: 0000-00003-2082-2768

Green synthesis of size-controlled silver nanoparticles and their anti-cancer potentiality

M. F. Kabir[a,b*], M. Z. Rahman[c], J. Ferdousy[d], M. Chalid[b], A. K. M Atique Ullah[e], M. Foysal[d], I. M. Razzakul[a], M. M. Rahman[c]

[a]*Material Science Division, Japan Advanced Institute of Science and Technology (JAIST)*
[b]*Health Physics Division, Bangladesh Atomic Energy Commission Dhaka, Dhaka-1000, Bangladesh*
[c]*Dept. of Physics, University of Dhaka, Dhaka-1000, Bangladesh*
[d]*Dept. of EEE, Green University of Bangladesh, Dhaka-1207, Bangladesh*
[e]*Chemistry Division, Bangladesh Atomic Energy Commission Dhaka, Dhaka-1000, Bangladesh*

Abstract

Silver nanoparticles have garnered attention in biomedical research due to their unique physicochemical properties, such as high surface area and antimicrobial activity. In the context of cancer research, silver nanoparticles have been explored for their potential in targeted drug delivery and therapeutic applications, demonstrating promising results in inhibiting cancer cell proliferation and inducing apoptosis. In the current investigation, Ag-NPs were effectively produced by reducing silver ions by employing the leaf extract of *Artocarpus heterophyllus* as a source of reducing and capping agents. By altering the quantity of the silver nitrate solution, we successfully synthesized three distinct kinds of Ag-nanoparticles that were mediated by *Artocarpus heterophyllus* leaf extract. The X-ray diffraction (XRD) analysis first confirmed the formation of metallic silver, where peaks were found at fixed angles. XRD method was also used to validate the crystal geometry of the Ag-NPs, revealing that the Ag-NPs had a face-cantered cubic structure. The calculated average crystallite sizes of Sample-1 Ag-NPs, Sample-2 Ag-NPs, and Sample-3 Ag-NPs were 20.34 nm, 16.99 nm, and 18.88 nm, respectively. Ag-NPs were also confirmed from EDX analysis and firm Ag peaks, including several organic compound peaks. The nanoparticle's range was between 120 nm and 220 nm, and the average particle size was near 170 nm, as found in the SEM image, and accumulation was observed in the SEM image. Using Fourier Transform Infrared (FT-IR) spectroscopy, we determined the functional groups of organic compounds that might be responsible for reducing agents and the presence of capping agents on the surface of Ag-NPs. The cell viability test was used to assess the cytotoxicity using the HeLa cell, a human carcinoma cell. The results revealed that the produced Ag-NPs demonstrated toxicity against carcinoma cells.

Keywords: Ag NPs, *Artocarpus heterophyllus*, cytotoxicity, HeLa cell, anti-cancer agent

1. Introduction

Nanotechnology is a promising multidisciplinary branch of study that provides nanoscale materials with the potential for use in various scientific domains, including engineering, mechanical engineering, catalysis, photonics, atomic processing, and essential materials [1, 2]. The quantum size effect causes it to display new and enhanced features and a vast surface area-to-volume ratio [3]. This is the most significant property responsible for the widespread usage of nanomaterials [3]. A broad range of biological characteristics, such as antiviral, anticancer, antibacterial, and antifungal activities, is present in green synthesized Ag-NPs, making them economical and environmentally benign [4]. Especially in biology, nanoparticles play a significant role due to their attractive physicochemical properties [5]. If the barrier ability of the skin was compromised, then silver nanoparticles (Ag-NPs) may pass through it at a rate ranging from 0.2 to 2 percent [6]. Several in vitro and in vivo investigations have shown that exposure to Ag-NPs may cause toxicity in organisms [7,8]. In addition, Ag-NPs' cytotoxicity effects on A-549, NIH-3T3, PC12, and HepG2 cell lines have been published in the scientific literature [9]. Besides, each year, millions of people worldwide are diagnosed with cancer [10]. The significant burden of most chemotherapeutic approaches to cancer treatment is that most of them are non-specific. Therapeutic, generally cytotoxic drugs are controlled intravenously, prompting total appropriation [11]. In this case, Ag-NPs can play a significant role as anti-cancer agents by providing their cytotoxic effects [12]. In addition, the antibacterial activity in Ag-NPs might facilitate their safe application in nutritional supplements, food packaging, cosmetics, and acne treatment products [13,14]. Designing nanoparticles that contribute to creating effective nanomaterials is one of the most significant means of combating antibiotic resistance [14]. Because of their large surface area bound to the cell surface, smaller Ag-NPs have more antibacterial action [15]. As a result, developing a method for manufacturing silver Ag-NPs that combines low toxicity with solid antibacterial activity is essential to ensure that these particles may be used without posing a risk to human health. So many chemicals and physical processes have been established to synthesiseAg-NPs. Chemical reduction [13], electrochemical [16], and sonochemical [17] are some of such synthesis processes. All of these methods are popular for the synthesis of Ag-NPs. However, these technologies cannot circumvent the need to use hazardous compounds in the synthesis procedure, which involves generating large amounts of dangerous by-products [18]. As a result of the widespread use of noble metal nanoparticles, such as silver and gold nanoparticles, in human-contact areas, it is of the utmost importance to develop what is known as "green chemistry," which entails the creation of nanoparticles in a way that is clean, non-toxic, and friendly to the

environment [19]. As a result of slower kinetics, more significant excitation, control over crystal development and stability, and cost-effectiveness, biological synthesis techniques have paved the way for the "greener synthesis" of nanoparticles [20]. Compared to chemical and physical approaches, natural nanoparticle synthesis methods have several advantages, including being more affordable, environmentally benign, and suitable for large production [20, 21]. "Green synthesis" of Ag-NPs was primarily reported by Gardea-Torresdey et al. [22]. The thriving green synthesis might be a contender to replace the conventional chemical production of Ag-NPs. The biologically synthesized Ag-NPs are biocompatible and can be safely used for various therapeutic applications. No report on Artocarpus heterophyllus leaf extract mediated Ag NPs size dependent anti-cancer activity. However, in this research, we used Artocarpus heterophyllus for synthesizing Ag-NPs. Artocarpus heterophyllus is the national fruit of Bangladesh. It might contain organic compounds, namely vitamins A, C, and E, with high glucosinolate compounds [23]. Moreover, Artocarpus heterophyllus grows almost yearly in Bangladesh and the Indian subcontinent. Therefore, the leaf extract of Artocarpus heterophyllus might be a possible option for use as a source of reducing and capping agents in the environmentally friendly manufacture of Ag-NPs.

2. Materials and Methods

2.1 *Chemicals and reagents*

Analytical grade types of chemicals were utilized in this study without any additional processing. To create the necessary solutions for this task, deionized water, also known as DI water, which has a resistivity of 18 MΩ-cm, is employed as a solvent. The chemicals and reagents utilized in this study include $AgNO_3$ (Merck, Germany), Artocarpus heterophyllus (known as Jackfruit) leaf, Dulbacos enhanced eagle's medium (DMEM) (Sigma, St. Louis, MO, USA), HeLa cell (American category culture collection, USA and Canada), etc.

2.2 *Preparation of leaf extract*

A few recently shed leaves of *Artocarpus heterophyllus* were gathered from the region immediately around the Dhaka University campus. After that, we removed the dust particles by washing them with tap water and rinsing them with deionized water. Furthermore, moisture was removed by drying them in an oven set at 60 °C and crushed into a powder. The plant extract was made by combining 10 g of plant extract with 200 mL of distilled water in a conical flask. Then the solution was mixed for 1 h at 80 °C, then centrifuged at room temperature for 30 min at 4000 rpm. After separating the supernatant, the liquid was filtered using Whatman No. 1 filter paper. Finally, the solution converted silver ions (Ag^+) into Ag-NPs. The temperature of the leaf extract

kept in the refrigerator was 4 °C. At each stage of the experiment, sterile conditions were maintained to ensure that the findings were reliable and accurate to prevent the introduction of any contamination.

An aqueous solution of 50 mM, 100 mM, and 200 mM silver nitrate was prepared in 200 mL conical flasks. For convenience, we marked the synthesized Ag-NPs using 50 mM silver nitrate solution as Sample-1, 100 mM as Sample-2, and 200 mM as Sample-3. For a better reaction, we took the silver nitrate solution in a beaker, and 50 mL leaf extract was added dropwise to reduce Ag^+ ions for each type of silver nitrate solution. The mixture was stirred for 60 min with a magnetic stirrer at 90 °C. Meanwhile, the gradual transformation of the mixture's colour from a pale yellowish-brown to a reddish-brown to a colloidal brown was seen and recorded at regular intervals. All the procedures were separately performed with each type of silver nitrate solution.

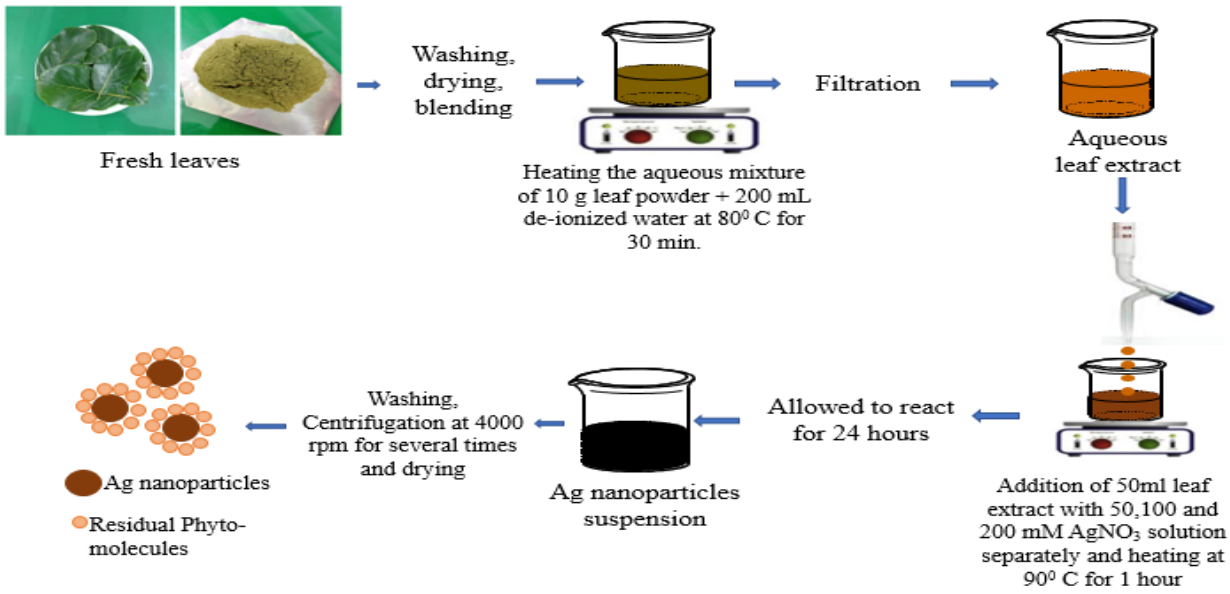

Figure 1: Schematic representation of silver nanoparticle synthesis process.

3. Results and discussion

3.1 *X-ray diffraction (XRD) analysis*

Using the XRD method and the associated XRD patterns, the crystalline nature of the green-produced Ag-NPs was substantiated. Fig. 2 showed the XRD patterns of Ag-NPs synthesized from the reduction of Ag^+ using leaf extract of Artocarpus heterophyllus at three different concentrations of silver nitrate solution. The diffraction peaks attained around the 2θ values of 38.05°, 44.33°, 64.38°, and 77.33° were matched to the planes of (111), (200), (220), and (311), correspondingly demonstrating the face-centred cubic (fcc) silver in accordance with the reference standard JCPDS Card No. 87-0720 [24]. In some cases, the diffraction peaks were shifted slightly

from the standard patterns, possibly due to the surface encapsulation of Ag-NPs [25]. The XRD patterns also showed that the relative intensity of the (111) diffraction peaks in Fig.2 is higher than the others. This result indicated that the synthesized Ag-NPs in our work were enriched in (111) facets. It is noteworthy that no unwanted peak was visualized in our synthesized Ag-NPs. This phenomenon indicates the formation of almost pure Ag-NPs. The structural parameters calculated from the XRD patterns for all three types of particles are summarized in Table 1. The crystallite size of Ag-NPs has been estimated using the Debye–Scherrer approximation: $D=k\lambda/\beta Cos\theta$ where "D is the average crystalline size, k is a geometric factor (0.9), λ is the wavelength of the X-ray radiation source, and β is the FWHM (full-width at half maximum) of the XRD peak at the angle of diffraction (θ)" [25]. The calculated average crystallite sizes of Sample-1 Ag-NPs, Sample-2 Ag-NPs, and Sample-3 Ag-NPs were 20.34 nm, 16.99 nm, and 18.88 nm, respectively.

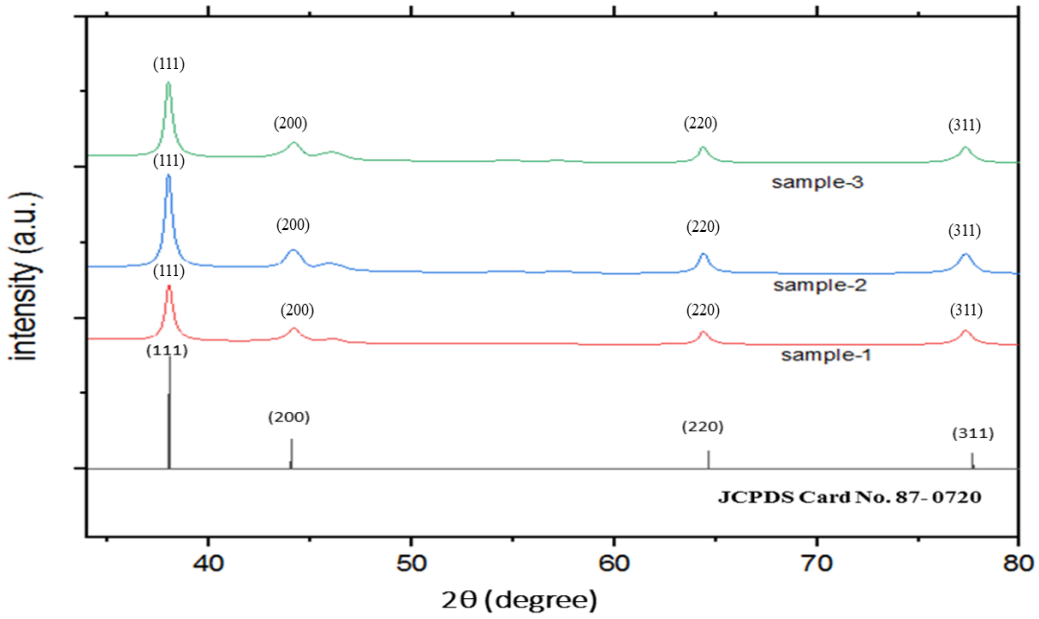

Figure 2: XRD patterns of synthesized Ag-NPs using three different concentrations of silver nitrate solution.

Table 1: The structural parameters of three different concentrated silver nitrate solutions-mediated synthesized Ag NPs were obtained from the XRD analysis

Silver nanoparticles	**Plane (h k l)**	**FWHM (deg.)**	**Crystallite Size, D (nm)**	**Average Crystallite Size (nm)**
Sample-1	111	0.4088	21.47	20.34
	200	0.4826	18.56	
	220	0.4351	22.54	
	311	0.5654	18.80	
Sample-2	111	0.3882	22.61	16.99
	200	0.8501	10.54	
	220	0.4993	19.64	
	311	0.7005	15.17	
Sample 3	111	0.3953	22.20	18.88
	200	0.7747	11.56	
	220	0.4501	21.79	
	311	0.5327	19.95	

3.2 *EDX analysis*

Strong indications of silver atoms were seen in the EDX profile. The existence of Ag NPs was shown by the prominent signal peak in the EDX spectrum at 3.25 KeV, which was characteristic of the absorption of silver Nano crystallites [24]. Interestingly, other components, including C, Cl, N, and O, were also found. The organic molecules from the extract that were absorbed on the surface of Ag NPs and played a critical role in Ag NPs reduction and stability were most likely connected with C and O [25].

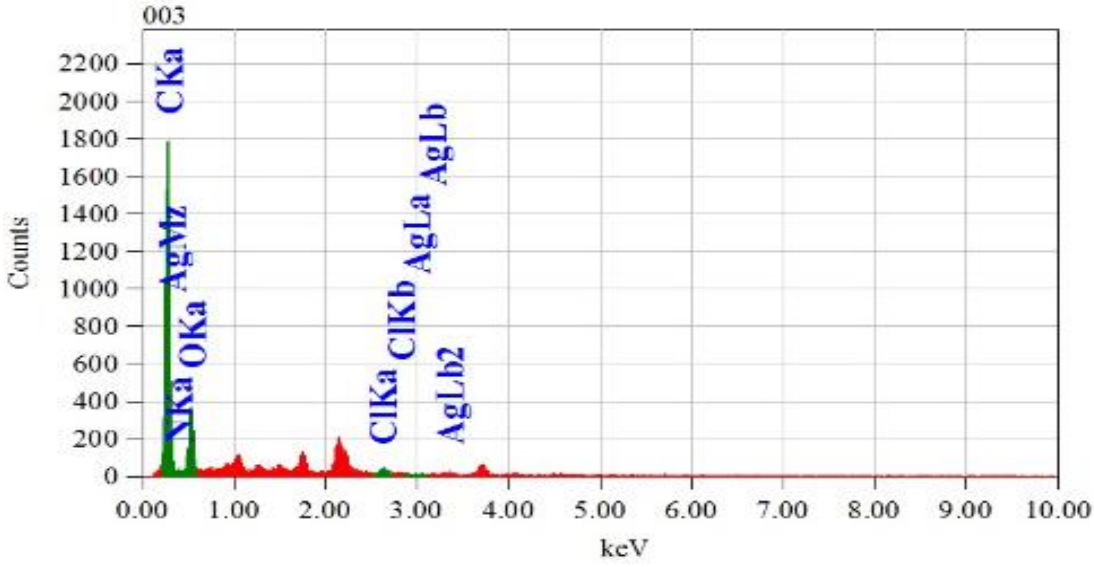

Figure 3: EDX image (for Sample 2) showing the presence of Ag NPs and bioorganic components from Artocarpus heterophyllus leaf extract.

The leaf extract solution also contained Cl [25–26]. Sample-1 and sample-3 had somewhat lower and greater concentrations, respectively. Only sample 2 was examined using EDS in this experiment. Since the three samples were all created using the same method, it seems sensible that they would have comparable components. Examining the sample-2 EDS result makes it simple to make predictions regarding sample-1 and sample-3.

3.3 *SEM micrographs analysis*

Scanning electron microscopy (SEM) was used to observe the surface morphology of the artificially produced silver nanoparticles (sample-2), and the results are shown in Figure 4. The scanning electron micrograph of silver nanoparticles (Ag NPs) showed unmistakably that the artificially produced Ag NPs were aggregated into dispersed clusters. The size distribution of the produced Ag NPs was roughly 120 nm to 220 nm, and the average particle size was 170 nm. The formation of the big particles that were seen most likely included the aggregation of several smaller particles [26].

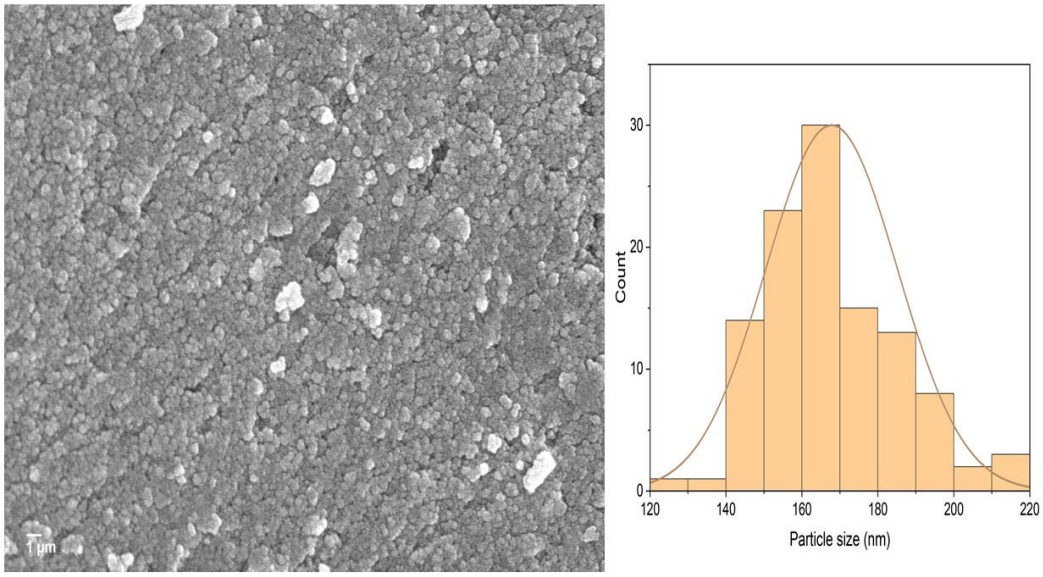

Figure 4: SEM micrographs of the biosynthesized Ag NPs (sample-2)

The massive particles may be eradicated using the heat treatment method. Other researchers also reported a similar phenomenon [26–27]. The fact that there was lower agglomeration may be because capping agents are present on the Ag NPs' surface; this was demonstrated both by the EDX and the FT-IR tests. Several characteristics working together typically determine the nanoparticle size range and size distribution. An essential factor to consider for size management is the silver nitrate solution ($AgNO_3$) concentration. On the other hand, the quantity of leaf extract solution used and its concentration may significantly impact particle size regulation. In this experiment, the scanning electron microscope (SEM) was only used to examine sample 2 since the concentration of samples 1 and 3 were, respectively, somewhat lower and higher. This lower and higher concentration might potentially increase or decrease the particle size. However, our primary objective was determining the cytotoxicity of concentration variation-mediated Ag NPs. The same method was used to generate all three samples, and the particle size distribution may be altered by adjusting the amount of $AgNO_3$ in the mixture. Finally, by analyzing the results of the SEM experiment performed on sample 2, it is possible to make an accurate prediction about the nanoparticle size of samples 1 and 2.

3.4 *Fourier transform infrared (FT-IR) spectroscopy*

FT-IR spectra were recorded for three different samples of synthesized Ag-nanoparticles, respectively, between wave numbers of 400 – 4000 cm^{-1}, to recognize the conceivable biomolecules responsible for reducing Ag^+ into Ag-NPs and their conjugation with the synthesized Ag-NPs that were shown in Fig.5. In Table-2, *Artocarpus heterophyllus* leaf extract-mediated

synthesized Ag-NPs, three firm peaks appeared for each sample which represents the stretching vibration bands of-C–O–C-, –C=O, and –OH, respectively [27,28]. Moreover, Weaker peaks also appeared, which specified the stretching vibration bands of -C–N of the amine, -C=C-, and-C–H, respectively [29,30].

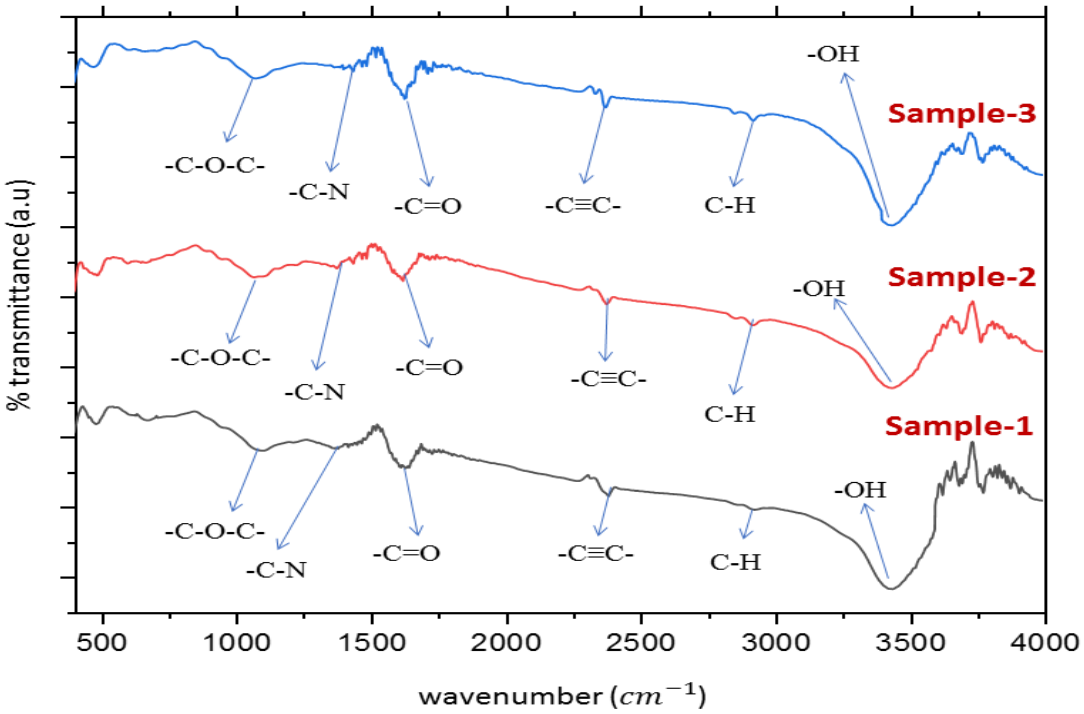

Figure 5: FT-IR spectra of Artocarpus heterophyllus leaf aqueous extract mediated synthesized Ag-NPs of sample-1, sample-2, and sample-3.

These bands were like the bands of *Artocarpus heterophyllus* aqueous leaf extract [29]. The FT-IR spectra of the three different concentrated synthesized Ag-NPs indicate that similar functional groups are present in the leaf extract and all the synthesized Ag-NPs. However, the peaks were shifted slightly, and the peak intensities were found to be increased for Ag-NPs, suggesting the condensation of the biomolecules on the surface results in the encapsulation of Ag-NPs with biomolecules.

Table 2: The structural parameters of three different concentrated silver nitrate solutions-mediated synthesized Ag NPs were obtained from the XRD analysis

Sample number	**Peaks position Wave number (cm^{-1})**	**Functional groups**	**References**
Sample-1	1098 cm^{-1}, 1626 cm^{-1}, and 3433 cm^{-1}	Stretching vibration bands of-C–O–C-, –C=O, and –OH respectively	[26, 27]
sample-2	1077 cm^{-1}, 1612 cm^{-1}, and 3440 cm^{-1}		
sample-3	1084 cm^{-1}, 1625 cm^{-1}, and 3438 cm^{-1}		
Sample-1	Weaker peaks appeared at 1366 cm^{-1}, 2386 cm^{-1}, and 2933 cm^{-1}	Specifying the stretching vibration bands of -C–N of the amine, -C=C-, and-C–H, respectively	[28, 29]
sample-2,	Weaker peaks appeared at1358 cm^{-1}, 2367 cm^{-1}, and 2933 cm^{-1}		
sample-3	Weaker peaks appeared at 1410 cm^{-1}, 2378 cm^{-1}, and 2927 cm^{-1} for		

3.5 *Cytotoxicity of Ag-NPs against cancerous cell*

The cell viability experiment assessed the cytotoxicity of the three concentrated synthesized Ag-NPs. HeLa cell line, a human cervical carcinoma cell line, was taken as a model cell. The synthesized Ag-NPs were then exposed to the selected cell lines at a 100 mg/L concentration. The phase-contrast microscopic pictures of Ag-NPs persuaded cytomorphological variations and growth inhibition of the cell lines with control. At three unlike concentrated synthesized Ag-NPs were shown in Fig.6. From the investigation of the cytotoxicity assay, it was found that the synthesized Ag-NPs were toxic, which was evidenced by the change of cytomorphology, indicating the decrease in cell viability. The cytotoxicity of the sample-1 Ag-NPs. Sample-2 Ag-NPs and sample-3 Ag-NPs against carcinoma cells were slightly varied. In the present study, sample -1 and sample-2 Ag-NPs were more toxic than sample-3 in table-3. Ag-NPs cytotoxicity has been widely studied. However, the specific processes by which Ag-NPs cause cell death are still largely unknown since cytotoxicity differs from cell to cell and NPs to NPs. Ag-NPs cytotoxicity has primarily been attributed to the disrupted antioxidant system and increased oxidative stress at the cellular level. Oxidative stress causes damage to the mitochondrial and plasma membranes, as well as to cellular proteins, lipids, and DNA, which ultimately results in

cell death and electronic chain dysfunction. The cytotoxicity shown in the current investigation may result from cellular harm caused by oxidative stress [30]. Additionally, the interaction of the encapsulating chemicals with the carcinoma cell may cause sample-1 and sample-2 increased cytotoxicity. The nanoparticles' size may impact cell damage, and $AgNO_3$ concentration strongly correlates with nanoparticle size. Maybe a tiny particle size is ideal for lower $AgNO_3$ concentrations, and cancer cell destruction is probably better suited to a small particle size.

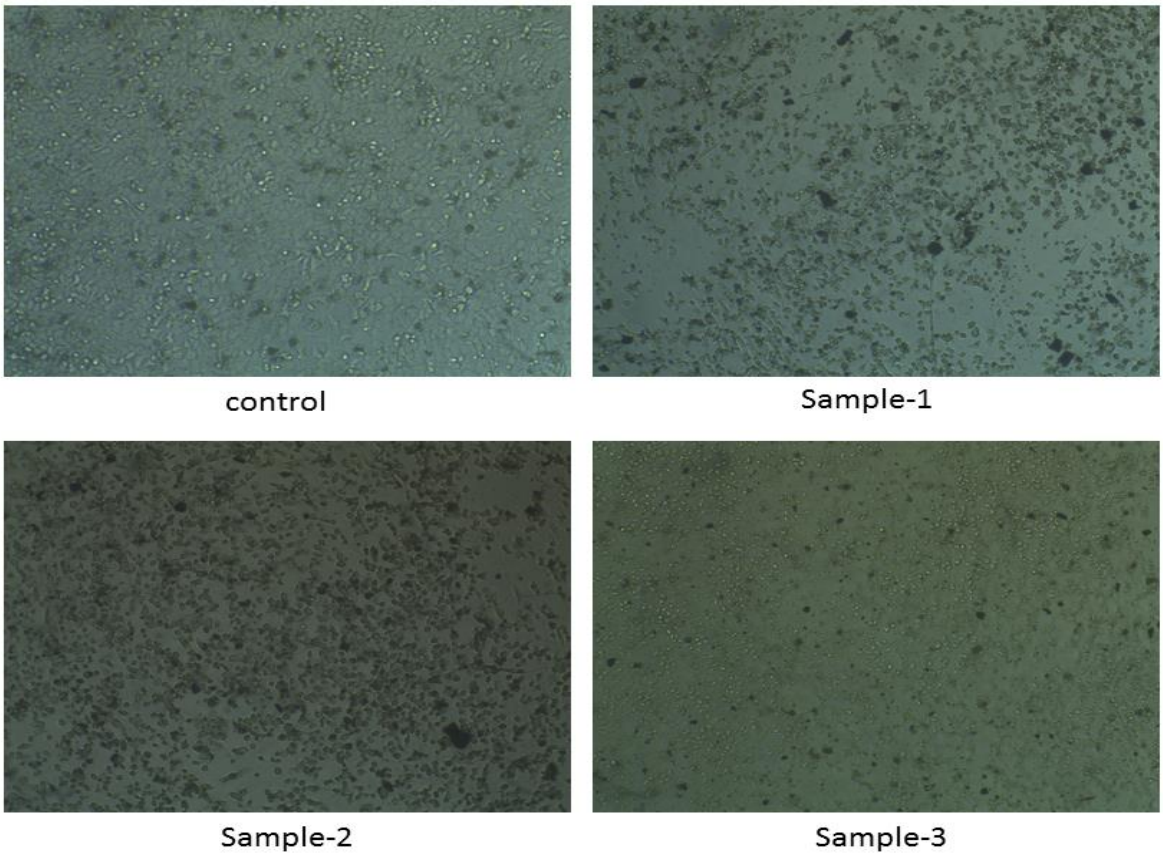

Figure 6: Phase contrasts microscopic images of the sample-1 Ag-NPs. Sample-2 Ag-NPs and sample-3 Ag-NPs induced cytomorphological changes and growth inhibition of cancerous HeLa cell line with control.

Table 3: Cytotoxicity of three different concentrated silver nitrate mediated synthesized Ag-NPs obtained from cell viability assay

Sample ID	Survival of HeLa Cells (%)	Remarks
Control	100%	Cytotoxicity was observed on the HeLa cell line
1	<5%	
2	<5%	
3	10%-20%	

4. Conclusions

In the current research, silver nanoparticles (Ag NPs) were effectively produced by the reduction of silver ions (Ag^+) with the leaf extract of *Artocarpus heterophyllus* (Jackfruit), which served as the reducing agent. It is also used as both a capping and a stabilizing agent. *Artocarpus heterophyllus* leaf was chosen as it was available in the Indian Subcontinent and found around the year. Different biomolecules in the leaf extract, confirmed by the FT-IR analysis, acted as reducing and capping agents. The XRD analysis confirmed the crystallinity and formation of the biosynthesized Ag NPs and found them to be face-cantered cubic. Due to some constraints, the surface morphology, particle size, and size distribution could not be examined. From the cell viability measurements, it was found that Ag-NPs are toxic to HeLa cells. The synthesized Ag NPs were effective as an anti-cancerous agent against human cancer cells. The toxicity increased with a particular concentration (50 mM and 100 mM) of Ag NPs. On the other hand, sample 3 has shown lower effectiveness than the other two samples. The Ag-NPs particle size-dependent cytotoxicity can impact future research, and the relationship between several parameters and cytotoxicity can be striking for future research. Cell-damaging mechanism study is quite important to know the actual role of Ag NPs in cytotoxicity, and it could be a unique research topic in the near future.

Conflicts of interest

The authors declare that they have no conflict of interest.

Acknowledgements

The authors would like to acknowledge the Materials Science Division, Atomic Energy Centre Dhaka; Department of Physics, University of Dhaka; and Department of Glass and Ceramic Engineering, Bangladesh University of Engineering and Technology for their assistance for the characterization; School of Material Science, and Japan Advanced Institute of Science and Technology (JAIST) for their cooperation.

References

[1]. T.V. Duncan, Applications of nanotechnology in food packaging and food safety: barrier materials, antimicrobials and sensors. Journal of colloid and interface science. 363, 1-24 (2011).

[2]. C. Carlson, S. M. Hussain, A. M. Schrand, L. Braydich-Stolle, K. L. Hess, R. L. Jones, J. J. Schlager, Unique cellular interaction of silver nanoparticles: size-dependent generation of reactive oxygen species. The journal of physical chemistry B. 112,13608-13619 (2008).

[3]. M. Akter, A. A. Ullah, M. S. Rahaman, M. M. Rahman, M. T. Sikder, T. Hosokawa, T. Saito, M. Kurasaki, Stability enhancement of silver nanoparticles through surface encapsulation via a facile green synthesis approach and toxicity reduction. Journal of Inorganic and Organometallic Polymers and Materials. 30,956-1965 (2020).

[4]. R. Balachandar, R. Navaneethan, M. Biruntha, K. K. A. Kumar, M. Govarthanan, N. Karmegam, Antibacterial activity of silver nanoparticles phytosynthesized from Glochidion candolleanum leaves. Materials Letters. 311,131572-131583 (2022).

[5]. S. Dutta, B. N. Ganguly, Characterization of ZnO nanoparticles grown in presence of Folic acid template. Journal of nanobiotechnology. 10,1-10 (2012).

[6]. R. S. Patil, M. R. Kokate, S. S. Kolekar, Bioinspired synthesis of highly stabilized silver nanoparticles using Ocimum tenuiflorum leaf extract and their antibacterial activity. Spectrochimica Acta Part A: Molecular and Biomolecular Spectroscopy. 91, 234-238 (2012).

[7]. M. Akter, A. K. M. Atique Ullah, S. Banik, M. T. Sikder, T. Hosokawa, T. Saito, M. Kurasaki, Green synthesized silver nanoparticles-mediated cytotoxic effect in colorectal cancer cells: NF-κB signal induced apoptosis through autophagy. Biological Trace Element Research. 199, 3272-3286 (2021).

[8]. J. H. Sung, J. H. Ji, J. D Park, J. U. Yoon, D. S. Kim, K.S. Jeon,M. Y. Song, J. Jeong, B. S.

Han, J. H. Han, Y. H. Chung, Subchronic inhalation toxicity of silver nanoparticles. Toxicological sciences. 108, 452-461 (2009).

[9]. N. H. Rezazadeh, F. Buazar, S. Matroodi, Synergistic effects of combinatorial chitosan and polyphenol biomolecules on enhanced antibacterial activity of biofunctionalized silver nanoparticles. Scientific reports. 10, 1-13 (2020).

[10]. G. H. Palliyage, N. Hussein, M. Mimlitz, C. Weeder, M. H. A. Alnasser, S. Singh, A. Ekpenyong, A. K. Tiwari, H. Chauhan, Novel Curcumin-Resveratrol Solid Nanoparticles Synergistically Inhibit Proliferation of Melanoma Cells. Pharmaceutical Research. 38, 851-871 (2021).

[11]. B. Schaefer, M. Tobiasch, S. Wagner, B. Glodny, H. Tilg, M. Wolf, H. Zoller, Hypophosphatemia after intravenous iron therapy: comprehensive review of clinical findings and recommendations for management. Bone. 154, 116202-116213 (2022).

[12]. M. F. Kabir, A. A. Ullah, J. Ferdousy, M. M. Rahman, anticancer efficacy of biogenic silver nanoparticles in vitro. SN Applied Sciences. 2, 1-8 (2020).

[13]. X. U. Vu, T. T. T. Duong, T. T. H. Pham, D. K. Trinh, X. H. Nguyen, V. S. Dang, Synthesis and study of silver nanoparticles for antibacterial activity against Escherichia coli and Staphylococcus aureus. Advances in Natural Sciences: Nanoscience and Nanotechnology. 9, 025019 -025027 (2018).

[14]. R. S. Shinde, R. A. More, V. A. Adole, P.B. Koli, T. B. Pawar, B. S. Jagdale, B. S. Desale, Y. S. Sarnikar, Design, fabrication, antitubercular, antibacterial, antifungal and antioxidant study of silver doped ZnO and CuO nano candidates: A comparative pharmacological study. Current Research in Green and Sustainable Chemistry. 4,100138 -100147 (2021).

[15]. M. P. Patil, R. D. Singh, P. B. Koli, K. T. Patil, B. S. Jagdale, A. R. Tipare, G. D. Kim, Antibacterial potential of silver nanoparticles synthesized using Madhuca longifolia flower extract as a green resource. Microbial pathogenesis. 121, 184-189 (2018).

[16]. S. Ali, X. Chen, M. A. Shah, M. Ali, M. Zareef, M. Arslan, S. Ahmad, T. Jiao, H. Li, Q. Chen, The avenue of fruit wastes to worth for synthesis of silver and gold nanoparticles and their antimicrobial application against foodborne pathogens: A review. Food Chemistry. 359, 129912-129921 (2021).

[17]. M. Bagheri, M. Heydari, P. Sangpour, S. Rabieh, In situ green synthesis of cellulose nanocomposite films incorporated with silver/silver chloride particles: characterization and antibacterial performance. Chemical Papers. 76, 6223-6233 (2022).

[18]. W. Hao, R. Chen, Y. Zhang, Y. Wang, Y. Zhao, Triazine-Based Conjugated Microporous

Polymers for Efficient Hydrogen Production. ACS omega. 6, 23782-23787 (2021).

[19]. M. Kannan, K. Elango, T. Tamilnayagan, S. Preetha, G. Kasivelu, Impact of nanomaterials on beneficial insects in agricultural ecosystems. Nanotechnology for food, agriculture, and environment. 2, 379-393 (2020).

[20]. M. A. Rasool, G. K. Gautam, D. P. Panda, D. C. Sahu, Preparation, Characterisation and Antifungal activity of Gold Nanoparticles prepared with Fresh Extract of Aconitum heterophyllum leaves. Research Journal of Pharmacy and Technology. 15, 3245-3250 (2022).

[21]. A. M. A. Ullah, M. F. Kabir, M. Akter, A. N. Tamanna, A. Hossain, A. R. A. Tareq, M. N. I. Khan, A. F. Kibria, M. Kurasaki, M. M. Rahman, Green synthesis of bio-molecule encapsulated magnetic silver nanoparticles and their antibacterial activity. RSC advances. 8, 37176-37183 (2018).

[22]. D. A. Kusumaningtyas, H. Khoirudin, M. Tami, M. U. Sari, A. Nirsatmanto, A. D. Nugraheni, F. Nugroho, Eucalyptus Leaves as Potential Indicators of Gold Mine in Indonesia. Jurnal Penelitian Pendidikan IPA. 8, 45-50 (2022).

[23]. D. Decker, L. A. Kleczkowski, UDP-sugar producing pyrophosphorylases: distinct and essential enzymes with overlapping substrate specificities, providing de novo precursors for glycosylation reactions. Frontiers in Plant Science. 9, 1822-1833 (2019).

[24]. S.D. Doke, C. M. Patel, V. N. Lad, Improving performance of the synthesis of silica nanoparticles by surfactant-incorporated wet attrition milling. Silicon. 1,1-10 (2021).

[25]. P. Aswathi, J. E. Thoppil, Synthesis and physicochemical characterization of silver nanoparticles from the dye-yielding plants, Terminalia paniculata and Mallotus philippensis. Nanotechnology for Environmental Engineering. 1, 1-10 (2022).

[26]. L. Tabassam, M. J. Khan, S. Hussain, S. A. Khattak, S. K. Shah, A. S. Bhatti, Structural, optical and antimicrobial characteristics of ZnO green nanoparticles. Journal of Sol-Gel Science and Technology. 101, 401-410 (2022).

[27]. L. Xu, Z. Xu, X. Liao, A review of fruit juice authenticity assessments: Targeted and untargeted analyses. Critical Reviews in Food Science and Nutrition. 62, 6081-6102 (2022).

[28]. M. Akter, M. M. Rahman, A. A. Ullah, M. T. Sikder, T. Hosokawa, T. Saito, M. Kurasaki, Brassica rapa var. japonica leaf extract mediated green synthesis of crystalline silver nanoparticles and evaluation of their stability, cytotoxicity and antibacterial activity. Journal of Inorganic and Organometallic Polymers and Materials. 28, 1483-1493 (2018).

[29]. B. W. Stuart, G. E. Stan, A. C. Popa, M. J. Carrington, I. Zgura, M. Necsulescu, D. M. Grant, New solutions for combatting implant bacterial infection based on silver nano-dispersed and

gallium incorporated phosphate bioactive glass sputtered films: A preliminary study. Bioactive Materials. 8, 325-340 (2022).

[30]. M. Akter, M. T. Sikder, M. M. Rahman, A. A. Ullah, K. F. B. Hossain, S. Banik, T. Hosokawa, T. Saito, M. Kurasaki, A systematic review on silver nanoparticles-induced cytotoxicity: Physicochemical properties and perspectives. Journal of advanced research. 9, 1-16 (2018).